PRAMANA
— journal of
physics

Vol. 60, No. 4
April 2003
pp. 675–686

Dileptons in high-energy heavy-ion collisions

RALF RAPP
Department of Physics and Astronomy, State University of New York, Stony Brook, NY 11794-3800, USA

Abstract. The current status of our understanding of dilepton production in ultra-relativistic heavy-ion collisions is discussed with special emphasis on signals from the (approach towards) chirally restored and deconfined phases. In particular, recent results of the CERN-SPS low-energy runs are compared to model predictions and interpreted. Prospects for RHIC experiments are given.

Keywords. Heavy-ion collisions; dileptons; quark–gluon plasma; chiral symmetry restoration.

PACS Nos 25.75.-q; 12.38.Mh; 24.10.Pa

1. Introduction

The rich physics potential of electromagnetic observables (photons and dileptons) has been clearly demonstrated over the past decade of heavy-ion experiments, especially at the CERN-SPS. Although the final spectra constitute a superposition of emission from the entire space-time history of a nucleus–nucleus collision, the original idea [1] of identifying signals from (thermalized?!) hot and dense phases of strongly interacting matter could be realized. Indeed, an excess of radiation in central Pb(158 A·GeV)–Au and Pb(158 A·GeV)–Pb collisions as compared to baseline p–p and p–A measurements has consistently been observed, most prominently for electron pairs at low invariant mass ($M \leq$ 1 GeV) by CERES/NA45 [2], muon pairs at intermediate mass (1.5 GeV $\leq M \leq$ 3 GeV) by NA50 [3] and photons at transverse momenta $q_{\rm t} \gtrsim 1.5$ GeV by WA98 [4]. From the theoretical side it should be emphasized that both dilepton and photon emission rates of a thermal medium are based on the same quantity, i.e., the (imaginary part of the) correlation function of the electromagnetic (e.m.) current (or photon self energy), $\mathrm{Im}\,\Pi_{\rm em}$. Thus a consistent description of both photon and dilepton observables within a common approach (coupled with a realistic space-time evolution for a heavy-ion collision) is mandatory (see refs [5,6] for recent reviews). Whereas real photons are related to the $M^2 \to 0^+$ limit of $\Pi_{\rm em}$ [6a], the production of time-like photons (=dileptons) requires $M^2 > 0$. The latter therefore carry additional dynamical information as, e.g., encoded in the low-lying (nonperturbative) vector–meson ($J^P = 1^-$) resonance excitations (ρ, ω and ϕ) of the QCD vacuum. This renders the low-mass region an ideal regime to study pertinent in-medium effects in connection with (the approach towards) chiral symmetry restoration, as will be further detailed below. At invariant masses beyond 1.5 GeV, the e.m. correlator becomes perturbative in nature, characterized by a rather structureless continuum with a strength governed by free

$q\bar{q}$ with controllable corrections in the strong coupling α_s, temperature and density. With an approximately known emissivity the virtue of the probe resides in the magnitude of the signal as an indicator of the temperatures reached in the early stages. The same idea is the main motivation [7] behind direct photon measurements. There is, however, a subtle but important difference: the leading contribution to photon production is of order $\mathcal{O}(\alpha\alpha_s)$ ($\alpha = 1/137$: e.m. coupling constant), whereas the one for (intermediate-mass) dileptons is $\mathcal{O}(\alpha^2)$ and therefore under better theoretical control (albeit experimentally suppressed).

2. Electromagnetic radiation: Hadron gas vs. QGP

2.1 *Production rate and e.m. correlator in free space*

To leading order in α, the emission rate of lepton pairs l^+l^- ($l = e, \mu$) from thermally equilibrated matter per unit 4-volume and 4-momentum reads [8]

$$\frac{\mathrm{d}R^{\mathrm{therm}}_{l^+l^-}}{\mathrm{d}^4q} = -\frac{\alpha^2}{\pi^3 M^2}\, f^{\mathrm{Bose}}(q_0;T)\ \mathrm{Im}\,\Pi_{\mathrm{em}}(M,q;\mu_B;T) \tag{1}$$

($M^2 = q_0^2 - q^2$). The theoretical objective is to calculate the (thermal expectation value of the) correlation function of two e.m. currents,

$$\Pi^{\mu\nu}_{\mathrm{em}}(q_0,q) = \int \mathrm{d}^4y\ \mathrm{e}^{iq\cdot y}\ \langle 0|j^\mu_{\mathrm{em}}(y)\, j^\nu_{\mathrm{em}}(0)|0\rangle, \tag{2}$$

which, in principle, contains all orders in the strong interaction. In practice, one has to invoke approximations starting from either quark or hadronic degrees of freedom. Accordingly, the current operator takes the form

$$j^\mu_{\mathrm{em}} = \begin{cases} \frac{1}{\sqrt{2}} j^\mu_\rho + \frac{\sqrt{2}}{6} j^\mu_\omega - \frac{1}{3} j^\mu_\phi & \text{hadronic basis} \\ \sum\limits_q e_q \bar{q}\gamma^\mu q = \frac{2}{3}\bar{u}\gamma^\mu u - \frac{1}{3}\bar{d}\gamma^\mu d - \frac{1}{3}\bar{s}\gamma^\mu s & \text{quark basis.} \end{cases} \tag{3}$$

In free space, the 'transition' can be inferred from the famous $e^+e^- \to$ hadrons cross-section: at low invariant mass, $\sqrt{s} \equiv M \lesssim 1.2$ GeV, it is saturated by ρ, ω and ϕ mesons (vector dominance model = VDM), whereas beyond $M \simeq 1.5$ GeV, the cross section is determined by weakly correlated $q\bar{q}$ pairs with almost no impact from subsequent hadronization (until additional flavor thresholds are reached where nonperturbative bound state formation occurs). Thus, the e.m. correlation function may be decomposed as

$$\mathrm{Im}\,\Pi_{\mathrm{em}}(s) = \begin{cases} \sum\limits_{V=\rho,\omega,\phi} \left(\frac{m_V^2}{g_V}\right)^2\ \mathrm{Im}\,D_V(s), & s \le s_{\mathrm{dual}} \\ -\frac{s}{12\pi}\,(1 + \frac{\alpha_s(s)}{\pi} + \cdots)\, N_c \sum\limits_{q=u,d,s} (e_q)^2, & s \ge s_{\mathrm{dual}}\,. \end{cases} \tag{4}$$

For the investigation of medium effects through dilepton production, an important question is how the spontaneous breaking of chiral symmetry (SBCS) manifests itself in the

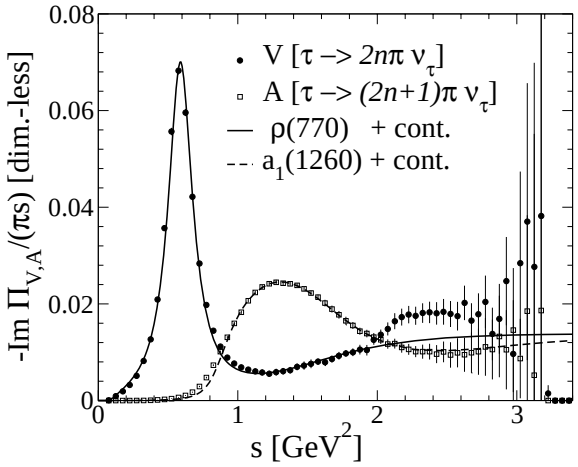

Figure 1. ALEPH data for axial/vector correlators as extracted from τ decays [9]. The curves are model calculations using ρ and a_1 resonances plus perturbative continua.

e.m. (or vector) correlator. A direct connection can be established in the isovector ($I = 1$) channel: at low mass, the pertinent hadronic current is entirely governed by the $\rho(770)$-meson which has a well-defined 'chiral partner' in the form of the $a_1(1260)$-meson, which itself saturates the low-mass part of the ($I = 1$) axial vector current. Recent data from τ decays by the ALEPH collaboration [9] nicely exhibit this feature, cf. figure 1. For $s \leq s_{\rm dual}$, the isovector hadronic (axial-) vector correlator can therefore be written as

$$\mathrm{Im}\Pi_{V,A}^{I=1}(s) = \begin{cases} \left(\frac{m_\rho^2}{g_\rho}\right)^2 \mathrm{Im}\, D_\rho(s), & IJ^P = 11^- \\ \left(\frac{m_{a_1}^2}{g_{a_1}}\right)^2 \mathrm{Im}\, D_{a_1}(s) - s f_\pi^2 \pi \delta(s - m_\pi^2), & IJ^P = 11^+ \,. \end{cases} \tag{5}$$

The difference between the two is the manifestation of SBCS in the QCD vacuum. Note the appearance of the pion pole contribution (the Goldstone boson of the symmetry breaking) with a residue given by the pion decay constant. At higher masses both correlators merge into a continuum value determined by perturbation theory:

$$\mathrm{Im}\,\Pi_{V,A}^{I=1} = -\frac{s}{12\pi}\left(1 + \frac{\alpha_s(s)}{\pi} + \cdots\right) N_c\,\frac{1}{2}\,, \tag{6}$$

i.e., beyond $s \simeq s_{\rm dual}$, effects due to SBCS no longer play a role.

Chiral symmetry breaking can be further quantified in terms of the Weinberg sum rules [10], which are energy-weighted moments of the difference between vector and axial vector correlators, e.g.,

$$f_\pi^2 = -\int \frac{\mathrm{d}s}{\pi s}(\mathrm{Im}\,\Pi_\rho - \mathrm{Im}\,\Pi_{a_1}). \tag{7}$$

Kapusta and Shuryak [11] have shown that these also hold in hot and dense matter which provides useful constraints on hadronic models. Chiral restoration obviously requires the

two correlators to degenerate over the entire mass range, i.e., $\mathrm{Im}\,\Pi_\rho(s) = \mathrm{Im}\,\Pi_{a_1}(s)$. How this is realized constitutes one of the main questions in the context of low-mass dilepton observables and related theoretical analyses. In this respect it is fortunate that the isovector channel dominates the strength in the e.m. correlator; for two flavors, e.g., the coefficient $\frac{1}{2}$ in eq. (6) amounts to ∼90% of the total emissivity (coefficient $\frac{5}{9}$ in eq. (4)).

2.2 *Medium effects*

Following the decomposition suggested in the previous section, a schematic overview of in-medium effects is given in table 1.

As emphasized before, the low-mass radiation from hadronic matter is well-suited to study in-medium modifications of light vector-mesons. Their vacuum properties are intimately related to the spontaneous chiral symmetry breaking; e.g., $M_V \simeq 2M_q$, with the constituent quark mass $M_q = 400$–500 MeV driven by the $\langle\bar{q}q\rangle$-condensate. Thus, even below T_c, medium modifications of vector mesons ought to be considered as a precursor phenomena of chiral restoration. Indeed, for low-mass lepton-pair emission the overall thermal Bose factor in eq. (1) induces a relatively moderate dependence on temperature, which is largely compensated by the volume increase of the expanding and cooling fireball in a heavy-ion collision. Thus, one is rather sensitive to medium effects in the spectral distributions themselves. These have been extensively studied in the literature. Starting points are typically effective, chirally invariant Lagrangians for hadronic interaction vertices with coupling constants and form factors determined by experiment. Based on the nuclear and finite-temperature many-body techniques one evaluates a vector-meson self-energy $\Sigma_\rho = \Sigma_{\rho\pi\pi} + \Sigma_{\rho M} + \Sigma_{\rho B}$ (similar for ω and ϕ) arising from interactions with the surrounding hot ($M = \pi, K, \rho, \ldots$) and dense ($B = N, \Lambda, \Delta, \ldots$) hadron gas (HG); $\Sigma_{\rho\pi\pi}$ incorporates medium modifications of the free $\rho \to \pi\pi$ decay. The generic outcome of such calculations is a strong increase of $|\mathrm{Im}\,\Sigma_\rho|$ with temperature and density, which broadens the ρ-meson spectral function, $\mathrm{Im}\,D_\rho$, beyond recognition of any resonance structure, cf. figure 2. At comparable densities, nuclear effects prevail over the ones induced by thermal pions (roughly speaking, interactions with pions are 'Goldstone'-protected).

In the invariant-mass window between 1 and 1.5 GeV, the main source of hadronic dilepton production is due to πa_1 annihilation [15]. This, in fact, can be understood as a pion-

Table 1. Summary of medium effects in thermal dilepton production.

	Hadron gas	Quark–gluon plasma
	In-medium ρ, ω, ϕ:	Perturbative QCD:
Low	Effective chiral Lagrangian + VDM	HTL-resummed $q\bar{q}$ annihilation [12]
mass	+ finite-T/-μ_B field theory [5]	+ LPM effect [13]
$M \lesssim 1$ GeV	$D_V = [M^2 - m_V^2 - \Sigma_V(M, q; \mu_B, T)]^{-1}$	non-pert. QCD:
		Gluon condensates ($T \gtrsim T_c$) [14]
Intermediate	$\pi a_1 \to l^+ l^-$ annihilation [15]	'Bare' α_s corrections
mass	$\hat{=}$ chiral V-A mixing [16]	to $q\bar{q}$ annihilation [18,19]
$M \gtrsim 1$ GeV	$\Pi_{V,A} = (1-\varepsilon)\,\Pi^0_{V,A} + \varepsilon\,\Pi^0_{A,V}$	order $\mathcal{O}\left(\alpha_s \frac{T^2}{M^2}\right)$

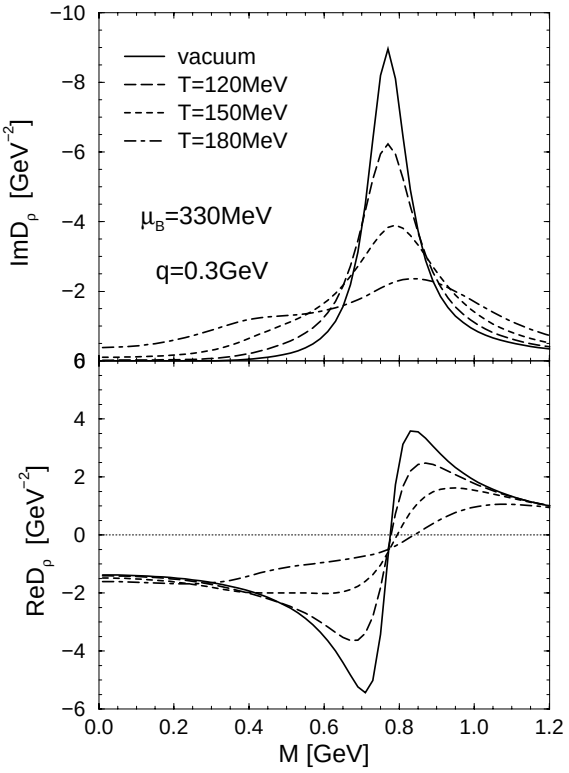

Figure 2. Real and imaginary part of the ρ-meson propagator [20] at finite temperatures and baryon densities.

induced mixing between the axial-vector and vector correlator (and vice versa) to lowest order in temperature, characterized by the parameter $\varepsilon = T^2/6f_\pi^2$ (chiral limit) [16]. When extrapolated to high temperatures, this 'chiral mixing' leads to a mutual degeneracy of V- and A-correlators not too far from the critical temperature as extracted from lattice gauge theory, $T_c = 170$–190 MeV.

Another line of treating medium effects employs chiral Lagrangians in mean-field approximation coupled with density-dependent corrections to masses and coupling constants. For example, within the so-called Brown–Rho scaling scenario [17], all hadron masses (except for Goldstone bosons) 'drop' with increasing temperature and density.

Turning to the QGP phase, it turns out that, at low mass, the correct leading-order in α_s result requires a resummation of thermal propagators accompanied by vertex corrections, which is achieved within the so-called hard thermal loop (HTL) framework [12]. Although the strong coupling constant g_s is not really small for practical applications in the QGP phase, $T \simeq (1$–$3)\ T_c$, the main qualitative result of a substantial enhancement of the rate towards small M (due to 'Bremsstrahlung'-type processes) should be rather robust. At higher masses, $M \gg T$, naive perturbation theory becomes applicable again, with moderate corrections [18,19].

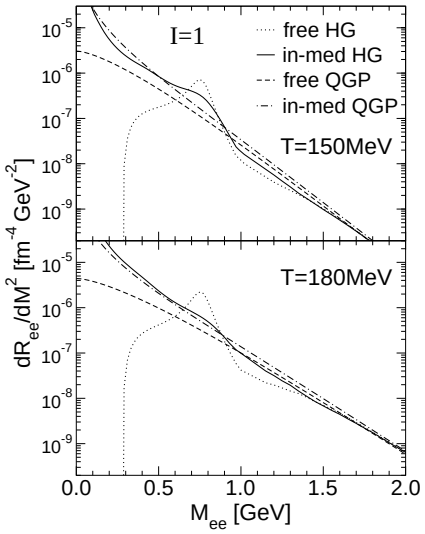

Figure 3. Equilibrium dilepton production rates from hadronic and QGP matter.

Figure 3 summarizes the various features graphically in terms of the three-momentum integrated production rate

$$\frac{\mathrm{d}R_{ee}}{\mathrm{d}M^2} = -\frac{\alpha^2}{\pi^3 M^2}\int \frac{\mathrm{d}^3q}{2q_0}\, f^{\mathrm{Bose}}(q_0;T)\ \mathrm{Im}\,\Pi_{\mathrm{em}}^{I=1}(M,q;\mu_{\mathrm{B}},T) \tag{8}$$

in the isovector channel, which amounts to a comparison of $\pi\pi$ annihilation (or ρ decays) in the HG vs. $q\bar{q}$ annihilation in the QGP phase. Starting from the free $\pi\pi$ and $q\bar{q}$ rates, which are obviously very different from each other, the respective in-medium corrections lead to (i) a characteristic low-mass enhancement in both the HG and QGP as well as (ii) ρ-resonance melting (around $M = m_\rho$) and chiral mixing (1 GeV$\leq M \leq$ 1.5 GeV) in the HG. As a result, the overall emissivities from the hadronic and quark–gluon phase look surprisingly similar around T_{c}, which has been interpreted as an in-medium reduction of the quark-hadron duality scale s_{dual} [20].

3. Dileptons at CERN-SPS energies

3.1 *Comparison to data*

Under the assumption that the highly excited matter formed in central heavy-ion reactions reaches thermal equilibrium at some typical formation time τ_0 ($\sim$1 fm/c at SPS), hydrodynamic or thermal fireball simulations are the appropriate framework for a consistent application of the thermal rates discussed in the previous section. Based on a fixed entropy per baryon as inferred from produced particle abundances, an isentropic thermodynamic trajectory $T(\mu_{\mathrm{B}})$ consistent with standard hadro-chemical freeze-out analyses [21,22] can be constructed including a phase transition from the QGP to HG. An important ingredient in the fireball expansion from chemical freeze-out, $(T_{\mathrm{ch}}, \mu_{\mathrm{B}}^{\mathrm{ch}})$ to the thermal one, $(T_{\mathrm{th}}, \mu_{\mathrm{B}}^{\mathrm{th}})$,

is the conservation of the observed particle multiplicities. This necessitates the build-up of finite meson-chemical potentials towards $T_{\rm th}$, e.g., $\mu_\pi^{\rm th} \simeq 60$–$80$ MeV at $E_{\rm lab} = 158$ A·GeV. The contribution of thermal radiation to observed spectra then takes the form

$$\frac{{\rm d}N_{l^+l^-}^{\rm thermal}}{{\rm d}M} = \int_{\tau_0}^{\tau_{fo}} {\rm d}\tau \, V_{\rm FB}(\tau) \int {\rm d}^3q \, \frac{M}{q_0} \, \frac{{\rm d}R_{l^+l^-}^{\rm thermal}}{{\rm d}^4q} \, Acc \, , \tag{9}$$

with $V_{\rm FB}$ the fireball volume and the factor *Acc* accounts for experimental acceptance cuts. In addition, contributions from long-lived hadron decays after freeze-out have to be included (the so-called 'cocktail' [2]).

An example of a thermal fireball calculation [20] plus cocktail is shown in the left panel of figure 4 and compared to CERES/NA45 data from Pb(158 A·GeV) + Au collisions. The enhancement over the cocktail cannot be described by adding free $\pi\pi$ annihilation within the fireball. With the strong medium effects as displayed in figure 2 (ρ-'melting'), a reasonable description is obtained. However, the assumption of a dropping ρ-mass also reproduces the data. The QGP contribution is small and insensitive to initial temperature and details of the phase transition construction. In the right panel of figure 4 the *predictions* of the same approach [20] are found to be consistent with the measurements at lower SPS energies (40 A·GeV) as well. In fact, despite the lower pion multiplicities, the calculations imply a slightly larger signal in the $M \simeq 0.4$ GeV region due to larger medium effects induced by higher baryon densities in the hadronic phase. This is in line with the trend of the data.

Another example of a low-mass dilepton prediction for the CERES 40 A·GeV run is shown in figure 5 in terms of a UrQMD transport calculation [24]. Closer inspection reveals that the Dalitz decay contributions $\omega \to \pi^0 e^+ e^-$ and $\eta \to \gamma e^+ e^-$, which are prevalent around $M \simeq 0.4$ GeV, are a factor of 3–4 above the standard hadrochemical cocktail [23].

Finally, we display in figure 6 a thermal fireball calculation [25] for the intermediate-mass dimuon spectra measured by NA50 in central Pb(158 A·GeV)+Pb. The 'dual' dilepton production rate based on eq. (4) has been folded over the same space-time evolution (modulo centrality) underlying the results of figure 4 [25a]. As anticipated, the yield is

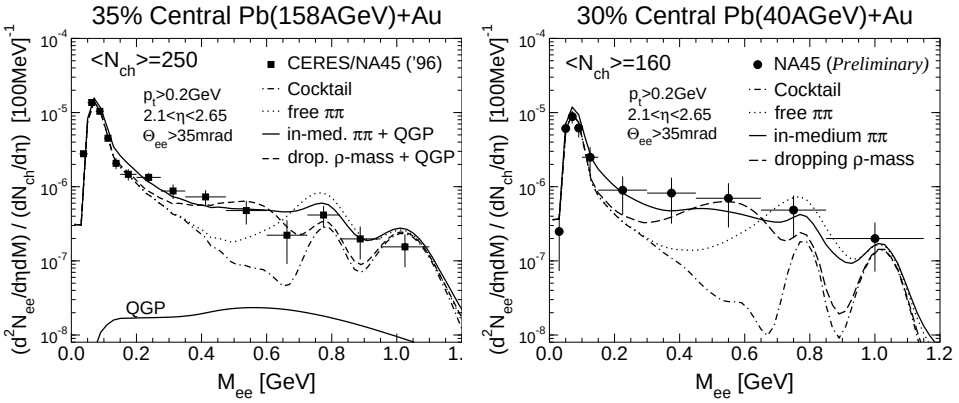

Figure 4. Thermal fireball calculations [20] for (semi-) central Pb + Au at 158 A·GeV and pertinent predictions for 40 A·GeV compared to CERES/NA45 data [2,23].

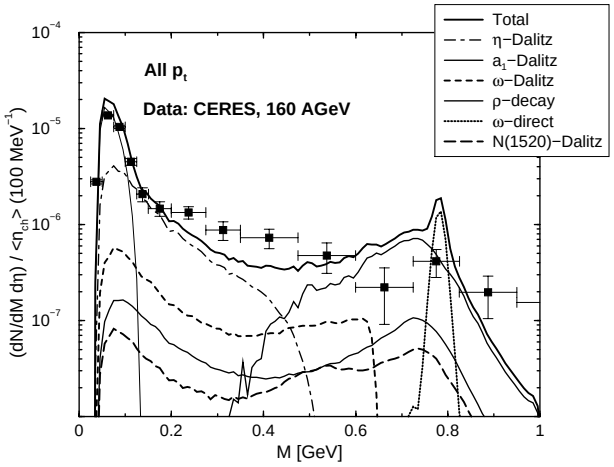

Figure 5. Transport calculations [24] for Pb(40 A·GeV) + Au. The 158 A·GeV data [2] have been included for orientation only.

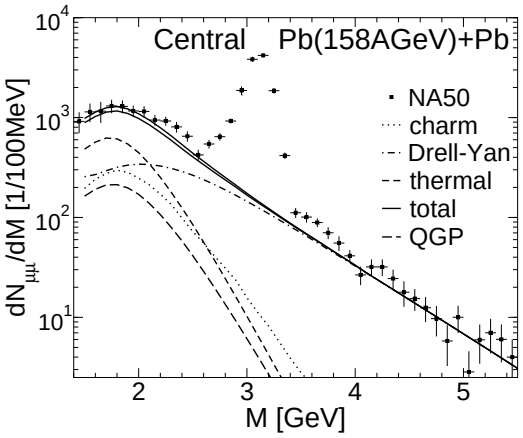

Figure 6. Thermal fireball calculations [25] compared to NA50 data [3]. Upper and lower total yields correspond to $T_0 = 220$ MeV and 195 MeV, respectively.

much more sensitive to the early phases with a significant part of the yield emerging from a QGP with preference for initial temperatures around $T_0 \simeq 220$ MeV.

3.2 *Consistency of models*

Let us first address the low-mass enhancement observed by CERES/NA45. Under the premise that the relative importance of baryon density effects around mid-rapidity increases towards lower collision energies (larger baryon stopping and lower initial temperatures), the indication for a large enhancement in the 40 A·GeV data suggests that its origin lies in baryon-driven in-medium effects as predicted within the many-body approach

of refs [26,20] (unless dramatic nonperturbative effects occur in the QGP phase close to T_c, which seems unlikely and finds no support in lattice results [27]). At the same time, transport calculations predicted very little effect from higher baryon density [24] and, in their present form, cannot describe the 158 A·GeV and 40 A·GeV data simultaneously.

Secondly, the NA50 dimuon enhancement at intermediate mass can be explained by thermal radiation within the same (fireball) evolution scenario [25] as the CERES data without additional parameters, albeit with a higher sensitivity to early (QGP) phases, as discussed above (see also refs [28,29]). In particular, an 'anomalous' open-charm enhancement (over the expectation from N–N collision scaling) is not required. In fact, the J/Ψ data of NA50 [30] also follow within a common framework [31] which combines suppression in a QGP and thermal production at T_c [32].

Finally a remark on thermal photons is in order [6]. The WA98 data [4] seem to require higher initial temperatures than the NA50 dimuons. However, photon production (both the hard component from N–N collisions as well as the QGP rates) has a nontrivial leading α_s-dependence which implies relatively larger uncertainties than in the dilepton sector. This equally applies to effects of (nuclear) k_t-broadening (Cronin effect), which might be larger than assumed in current calculations and thus responsible for (part of) the discrepancy.

3.3 *Chiral restoration*

Let us briefly elaborate on some recent developments.

In [33] the so-called 'vector manifestation' of chiral symmetry restoration has been suggested: within the hidden local symmetry framework, the chiral partner of the pion is identified with the longitudinal component of the ρ meson. When applied within a one-loop renormalization group evolution towards the symmetry restoration point, the ρ mass along with f_π and g_ρ go to zero. In particular, VDM does not hold at finite T.

Rather different results are obtained in ref. [34], where a linear $\sigma\pi\rho a_1$ model, consistently constructed to 1-loop order with realistic vacuum properties, has been applied at finite temperature. It is found that, even if the vacuum ρ mass at tree level is entirely given through the $\langle\bar{q}q\rangle$ condensate, the vanishing of the latter at T_c does not significantly impact $m_\rho(T_c)$ due to different (leading) temperature dependencies of the two quantities [16]. The main effect was rather a substantial broadening of both the ρ and a_1 spectral functions. This is not inconsistent with the chiral restoration scenario put forward in ref. [20], where the degeneracy of vector and axial-vector correlators is realized through the in-medium reduction of the quark-hadron duality threshold.

The relative importance of baryonic effects in 'melting' the ρ resonance calls for a better understanding of their relation to chiral symmetry. A possible scheme is illustrated in figure 7, which combines pionic S-wave excitations connecting chiral partners with pionic

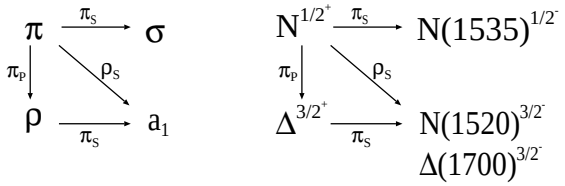

Figure 7. Interaction scheme combining chiral and resonance excitations.

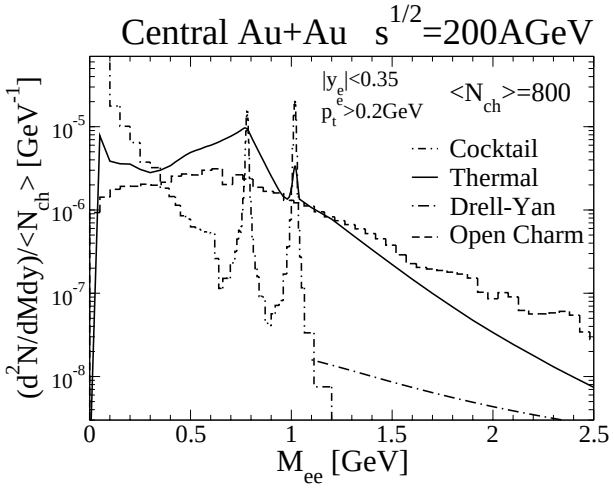

Figure 8. Dilepton spectra from central Au + Au collisions at full RHIC energy.

P-wave excitations representing hadronic resonance physics. In particular, the analogy between the mesonic (left panel) and baryonic (right panel) sector identifies the prominent role of the ρN *S*-wave resonances $N(1520)$ and $\Delta(1700)$.

4. Predictions for RHIC

The beginning of the collider era through the first operation of BNL-RHIC has opened a new energy frontier in heavy-ion physics. First dilepton data are expected from the second run of Au + Au (completed in November 2001) at the full energy of $\sqrt{s} = 200$ A·GeV.

Predictions for e^+e^- spectra in central Au + Au are summarized in figure 8 for the invariant-mass range from 0 to 2.5 GeV. The thermal contribution [35] has been evaluated within a fireball model with realistic values for the charged particle multiplicity [36] and an estimated $\bar{p}/p$-ratio of ∼75%. The radiation from the QGP phase (with initial temperature $T_0 \simeq 380$ MeV) dominates the thermal yield at masses $M \gtrsim 1.5$ GeV. Its detectability will critically depend on the contribution from correlated open-charm decays, which in figure 8 has been taken from a PHENIX event generator [37] which is based on an extrapolation of *N*–*N* collisions (using PYTHIA) at lower energies. If the spectrum of the *c*-quarks experiences significant softening (e.g., through energy loss in the QGP), the associated dilepton spectrum may be severely suppressed above $M = 2$ GeV or so [38], opening the window for the QGP signal. In the low-mass region, thermal radiation mostly originates from the hadronic phase and compares favorably to both open-charm and the hadronic decay cocktail after freeze-out [37] (here, subtraction of the combinatorial background will be the main experimental problem). In-medium modifications again 'melt' the ρ-resonance which drives the enhancement below $M \simeq 0.6$ GeV [38a]. Similar effects lead to an in-medium signal from ω-decays with an average width of ~ 50 MeV, almost seven times its vacuum value (less pronounced for ϕ).

5. Conclusions

Driven by exciting data, the theoretical and phenomenological analyses of dilepton production in high-energy reactions of heavy nuclei have undergone continuous progress with increasing consensus among most approaches. As for the low-mass region, the CERES/NA45 data at full SPS energy (158 A·GeV) require strong medium modifications of the ρ-meson indicating that one is indeed probing strong interaction matter in the vicinity of T_c (with small contributions from the QGP phase itself). The new 40 A·GeV data support the importance of baryon-driven effects, while their relation to chiral symmetry (especially for resonances) remains to be better understood. 'ρ-melting' with 'quark-hadron duality' towards T_c remains a viable scenario of chiral restoration. At intermediate masses, the NA50 enhancement consistently emerges from the same thermal source, but with significantly larger sensitivity to the QGP phase pointing at initial temperatures $T_0 \geq 200$ MeV. New exciting insights can be expected soon from PHENIX at RHIC, HADES at SIS and farther into the future from ALICE at LHC. This raises the hope of a systematic understanding of dilepton emissivities across the QCD phase diagram.

Acknowledgement

This work has been supported by the US-DOE grant DE-FG0288ER40388.

References

[1] E V Shuryak, *Phys. Rep.* **61**, 71 (1980)
[2] G Agakishiev *et al*, CERES/NA45 Collaboration, *Phys. Lett.* **B422**, 405 (1998)
[3] M C Abreu *et al*, NA50 Collaboration, *Euro. Phys J.* **C14**, 443 (2000)
[4] M M Aggarwal *et al*, WA98 Collaboration, *Phys. Rev. Lett.* **85**, 3595 (2000)
[5] R Rapp and J Wambach, *Adv. Nucl. Phys.* **25**, 1 (2000)
[6] T Peitzmann and M Thoma, hep-ph/0111114
[6a] The e.m. correlator is also directly relevant to studies of charge fluctuations. The fluctuation content of a locally thermalized system is directly proportional to the static space-like limit of Π_{em}
[7] J Alam, *Pramana – J. Phys.* **60**, 663 (2003)
[8] L McLerran and T Toimela, *Phys. Rev.* **D31**, 545 (1985)
[9] R Barate *et al*, ALEPH Collaboration, *Euro. Phys. J.* **C4**, 409 (1998)
[10] S Weinberg, *Phys. Rev. Lett.* **18**, 507 (1967)
[11] J I Kapusta and E V Shuryak, *Phys. Rev.* **D49**, 4694 (1994)
[12] E Braaten, R D Pisarski and T C Yuan, *Phys. Rev. Lett.* **64**, 2242 (1990)
[13] J Cleymans, V V Goloviznin and K Redlich, *Z. Phys.* **C59**, 495 (1993)
[14] C H Lee, J Wirstam, I Zahed and T H Hansson, *Phys. Lett.* **B448**, 168 (1999)
[15] G Q Li and C Gale, *Phys. Rev. Lett.* **81**, 1572 (1998)
[16] M Dey, V L Eletsky and B L Ioffe, *Phys. Lett.* **B252**, 620 (1990)
[17] G E Brown and M Rho, hep-ph/01031202
[18] T Altherr and P Aurenche, *Z. Phys.* **C45**, 99 (1989)
T Altherr and P V Ruuskanen, *Nucl. Phys.* **B380**, 377 (1992)
[19] J I Kapusta and S M H Wong, *Phys. Rev.* **C62**, 027901 (2000)

[20] R Rapp and J Wambach, *Euro. Phys. J.* **A6**, 415 (1999)
[21] P Braun-Munzinger, I Heppe and J Stachel, *Phys. Lett.* **465**, 15 (1999)
[22] F Becattini, J Cleymans, A Keranen, E Suhonen and K Redlich, hep-ph/0011322
[23] D Adamova *et al*, CERES/NA45 Collaboration, *Nucl. Phys.* **A698**, 253 (2001)
[24] M Bleicher, A K Dutt-Mazumder, C Gale, C M Ko and V Koch, hep-ph/0004044
[25] R Rapp and E V Shuryak, *Phys. Lett.* **B473**, 13 (2000)
[25a] Note that, the experimental fact that hadron production in e^+e^- annihilation follows statistical (thermal) model predictions justifies the use of the perturbative ('dual') rate in the intermediate mass region even in the hadronic phases of a heavy-ion collision: the thermal heat bath is the same state as produced in $e^+e^- \to$ hadrons, so that one can use time-reversal invariance to obtain the e^+e^- production rate
[26] R Rapp, G Chanfray and J Wambach, *Nucl. Phys.* **A617**, 472 (1997)
[27] F Karsch, E Laermann, P Petreczky, S Stickan and I Wetzorke, hep-lat/0110208
[28] K Gallmeister, B Kämpfer and O P Pavlenko, *Phys. Lett.* **B473**, 20 (2000)
[29] D K Srivastava, B Sinha, I Kvasnikowa and C Gale, *Nucl. Phys.* **A698**, 432 (2002)
[30] M C Abreu *et al*, NA50 Collaboration, *Phys. Lett.* **B477**, 28 (2000)
[31] L Grandchamp and R Rapp, *Phys. Lett.* **B523**, 60 (2001)
[32] P Braun-Munzinger and J Stachel, *Phys. Lett.* **B490**, 196 (2000)
[33] M Harada and K Yamawaki, *Phys. Rev. Lett.* **86**, 757 (2001)
[34] M Urban, M Buballa and J Wambach, hep-ph/0110005
[35] R Rapp, *Phys. Rev.* **C63**, 054907 (2001)
[36] B B Back *et al*, PHOBOS Collaboration, *Phys. Rev. Lett.* **88**, 022302 (2002)
[37] R Averbeck, private communication
[38] E V Shuryak, *Phys. Rev.* **C55**, 961 (1997)
[38a] Even with the rather small *net* baryon densities at mid-rapidities at RHIC, the copious abundance of baryon–antibaryon pairs contributes significantly to the broadening [35]